PROCEEDINGS OF SPIE

SPIEDigitalLibrary.org/conference-proceedings-of-spie

Pupillary sensor for ocular cranial nerve monitoring

Chambers, Rheagan, Quon, Nick, Slomka, Bridget, Martirosyan, Nikolay, Lemole, Michael, et al.

Rheagan Chambers, Nick Quon, Bridget Slomka, Nikolay Martirosyan, Michael Lemole Jr., Marek Romanowski, "Pupillary sensor for ocular cranial nerve monitoring," Proc. SPIE 11225, Clinical and Translational Neurophotonics 2020, 112250I (17 February 2020); doi: 10.1117/12.2542058

SPIE.

Event: SPIE BiOS, 2020, San Francisco, California, United States

Pupillary sensor for ocular cranial nerve monitoring

Rheagan Chambers[a], Nick Quon[a], Bridget Slomka[a], Nikolay Martirosyan[b], Michael Lemole[b], Marek Romanowski[a]
[a]Department of Biomedical Engineering, [b]Department of Neurosurgery
University of Arizona, Tucson AZ 85721

ABSTRACT

In humans, the pupillary light reflex (PLR) is the change in diameter of the pupil as a response to changes in light intensity. By quantitatively monitoring the pupillary light reflex, there is potential to gain diagnostic knowledge for patients in a variety of situations including those suffering from a traumatic brain injury as well as those undergoing invasive neurosurgery proximal to the optic nerves. To improve the diagnostic capabilities of the PLR, a novel pupillometer was developed. The pupillometer is intended for direct placement on the eye and allows for the continuous stimulation and monitoring of pupillary light reflexes. Tests on anesthetized rabbits demonstrate real-time data acquisition and display, including the pupil diameter and velocities of constriction and dilation. The sensor is in development for implementation as a clinical device to monitor the status of the oculomotor nerves, and may also find applications in the diagnostic assessment of traumatic brain injury or changes in intracranial pressure.

Keywords: pupillometer, cranial nerve, pupillary light response, traumatic brain injury, intracranial pressure, pupil, medical imaging, spherical aberration

1. INTRODUCTION

It has been proven that the pupillary light reflex (PLR) can provide useful information regarding the functionality of the human body. Specifically, the PLR can be monitored as an indicator of the health of the optic nerves during neurosurgery, episodes of increased intracranial pressure, and in circumstances of traumatic brain injury. One common theme is that the optic nerves, which control aspects of the PLR, produce abnormal PLR when injured or under increased pressure.

In the United States, traumatic brain injury (TBI) contributes up to 30% of all injury-related deaths.[1] In 2013, the U.S. reported approximately 2.5 million emergency department (ED) visits, 282,000 hospitalizations, and nearly 50,000 deaths attributed to TBI alone or in combination with other injuries.[1] The consequences of such an injury can affect all aspects of a person's life, including physical and mental abilities, emotions, or personality. The effects faced by those who survive a TBI may last for a few days or for the rest of their lives. Because there are a variety of symptoms and multiple severities of TBI, there is a significant need for gathering information about patient TBI status, as this knowledge will impact the care provided.

Similarly, incidences of increased intracranial pressure (ICP) also occur with varying symptoms, with some individuals showing none at all.[1] As increased pressure within ventricles of the brain correlates with high mortality, methods of monitoring ICP are critically important in clinical practice. Healthy adults experience a typical pressure range of 3-10 mmHg. For individuals with mild TBI, this pressure value could be in the range of 20-30 mmHg, and for this with moderate TBI this value is approximately 30-40 mmHg. Readings above this indicates severe TBI. An ICP of 40 mmHg or greater has been associated with a mortality rate of 65%.[2] It has been noted that, in individuals with an ICP of 60 mmHg, the mortality rate is 100%.[2]

Currently, the best method to determine presence of raise ICP is through direct invasive measurement. Techniques used to measure ICP include, but are not limited to, the use of an intraventricular catheter or an intraparenchymal probe. The ventricular catheter has been the gold standard since the 1960s.[3] To perform this technique, the patient must undergo a ventriculostomy. This procedure is performed under local anesthesia, and requires that a catheter be positioned through a burr hole to the ventricles of the brain and attached to an external strain gauge transducer to yield measurements of ICP.[4] While this procedure rarely has complications, it is invasive and has not been shown to improve patient outcomes.[4]

Evaluation of the pupillary light reflex can provide useful information about the integrity of cranial nerves for both sensory and motor tracts. There is also potential that it can provide an indirect measure of intracranial pressure, which

Clinical and Translational Neurophotonics 2020, edited by Steen J. Madsen, Victor X. D. Yang, Nitish V. Thakor
Proc. of SPIE Vol. 11225, 112250I · © 2020 SPIE · CCC code: 1605-7422/20/$21 · doi: 10.1117/12.2542058

can also be applied to TBI.[3] Quantitative parameters of the PLR, such as maximum and minimum pupil diameter, pupil constriction ratio, pupil constriction latency, and velocity of pupil diameter changes, are used to determine pupil reactivity. To gather this data, pupillometers seek to provide quantitative pupillary function information. The most basic device used for measuring pupil diameter is the Haab Scale. The device has black circles painted on its surface that gradually increase in size and are used as a comparison by holding it up to the subject's pupil.[5] This method requires an observer to visually compare the pupil to the reference circles and estimate the diameter of the patient's pupil. The current standard for reflex pupillometers today are hand-held devices whose design derives from 40-year-old technology. The measurements acquired with these devices are intermittent and require logistically difficult manipulations[6], such as manual opening of eyelid and measurement of the contralateral response. However, in the intensive care unit or operating room with critical or anesthetized patients, such manipulations are not always feasible. To address this medical need for a method of taking quantitative measurements of pupillary light reflex, we introduce a pupillary device that combines both light sources and a camera in a package that can be placed directly on the eye to continuously monitor the PLR and extract the amplitude, latency, and velocity in real time.

2. METHODOLOGY

2.1 Construction of the Pupillometer

The pupillary device was composed of several individual components. Transparent corneal shields were obtained from Kolberg Ocular Supplies, Inc (City State). The camera mount was designed in SolidWorks and manufactured using a 3D-printer. The camera was Awaiba's Naneye (now ams AG, Austria), a black & white 250x250 pixel 10-bit sensor, equipped with a wide-angle lens with an f-number of 2.4, a diagonal field of view 160° in air, and a working distance of 5 mm. The overall dimension of this wafer-level camera package is 1x1x1.4 mm, including the lens. For image acquisition we incorporated a near-infrared LED emitting at 850 nm, and for stimulation of PLR we used a white LED. The funnel-like 3D printed camera mount was adhered on the convex surface of the corneal shield with cyanoacrylate adhesive. Through the funnel structure, a miniature camera was affixed to the shield surface with polyvinyl alcohol to facilitate removal if needed. The LEDs were affixed on the portion of the funnel-shaped camera mount in contact with the shield. Electrical connections use 32 AWG wires which are bundled and exit through the cylindrical stem of the camera mount. The length of the wire bundle connecting the sensor to the electronic board is limited to 2 m, sufficient for working in live subjects. In all experiments, the data were collected using an interface board and Application Programming Interface (API) provided by Awaiba, both supporting communication via USB3 and applications developed in Microsoft Visual Studio.

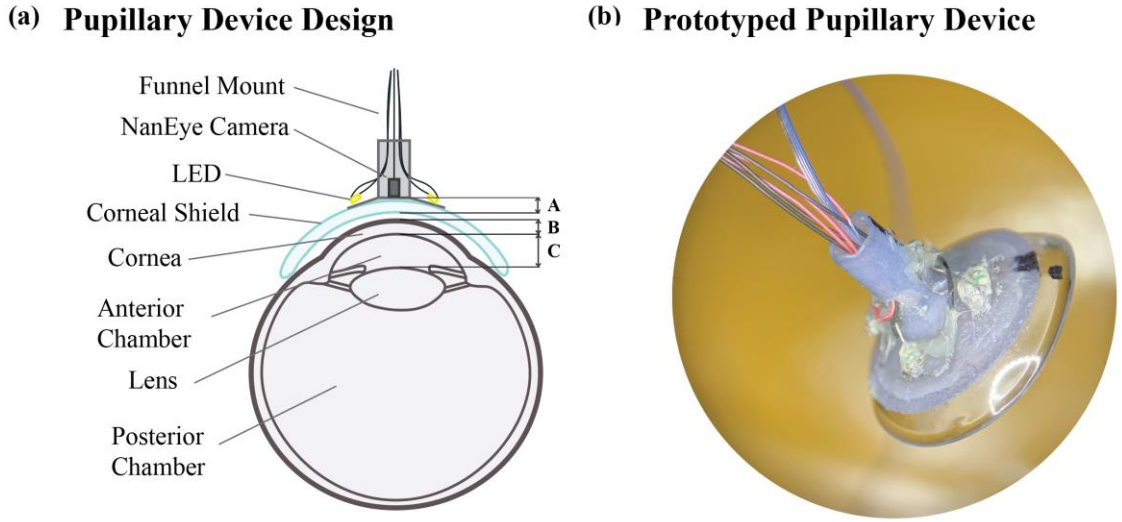

Figure 1. **(a)** 2-dimensional depiction of the proposed pupillometer on the eye when viewed as along the horizontal sagittal plane. **A** is the distance from the NanEye camera lens to the inner surface of the corneal shield, approximately 2 mm. **B** is the thickness of the cornea, 0.5 mm. **C** is distance from the inner surface of the cornea to the iris, 3.3 mm. **(b)** Photograph of the prototyped pupillometer.

2.2 Operational Code

Communication between the camera module and image processing was conducted in C++ using Microsoft Visual Studio 2017. Images were captured by the NanEye camera in the .jpeg format, sent to a PC via USB3 connection, and then processed using several image processing techniques with OpenCV. First, adaptive thresholding was conducted via the adaptiveThreshold function. This method allows the detection of the pupil to adapt to different illumination levels without intervention. To remove imperfections in the images captured, morphological transformations were conducted using morphologyEx. By use of the process of erosion, or receding edges and removing noise, followed by dilation, or increasing edge size, noise can be eliminated from the image. The image is then smoothed with a Gaussian filter, GaussianBlur, to eliminate high-frequency noise. Using Canny edge detection as well as blob detection via the SimpleBlobDetector algorithm within OpenCV, shapes can be detected based on several parameters. Detected masses, or blobs, were filtered largely by size and circularity. Following this phase of processing, the radius of the circle detected was determined by a program to estimate the center of the circle and then plot the distance from this center to the outer edge. To ensure that this process visually aligned with the images captured by the NanEye camera, the information regarding radius and center location was stored in a vector and superimposed in real-time on images as they were captured. The data were stored in a .dat file with two columns. The first column includes the time that the image was received, and the second column includes the diameter of the pupil detected with image processing. Following this processing, the data gathered in the .dat file was displayed graphically using a third-party library, Gnuplot. After processing and extraction of relevant data, the image was deleted and replaced by the next available frame from the NanEye camera, for which the process repeated.

2.3 Spherical Aberration

To calibrate the image acquisition system and assess its aberrations, targets consisting of concentric circles were printed with 1200x1200 dpi resolution. Several configurations were tested to represent the spatial arrangement of image acquisition. First, the sensor was centered on the printed target with air space between the two (A), and images were collected. Next, a plano-convex lens of 25 mm focal length, approximately representing the optical power of a cornea, was placed on a target and the sensor was then placed on the lens (B). After centering, images were captured for this condition. The next set up consisted of the same target, lens, and sensor configuration, but at the interface of the corneal shield and the lens, polyvinyl alcohol (PVA) was added as a lubricant (C), and images were recorded. In all of these configurations, the camera rested on the outer face of the corneal shield and images are captured through the shield. In the final configuration, a small hole was drilled through the corneal shield, such that the camera can be inserted through the shield and adhered flush with the inner surface of the shield. This configuration was then tested with the plano-convex lens with PVA (D) as the interface, and images were captured. Each image was then loaded in Adobe Photoshop 2017. Within Photoshop, the number of pixels from each concentric radius to the next was counted and recorded. These values were then transferred to MATLAB and graphed to determine the functions that could be used to correct for spherical aberration in each set up.

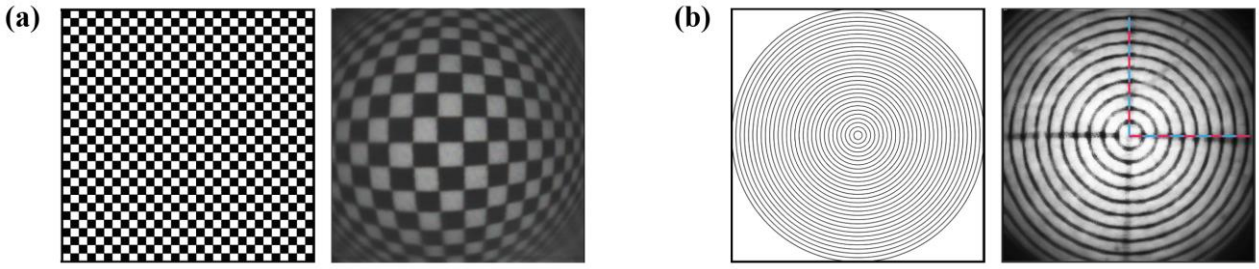

Figure 2. **(a)** The two images depict a checkerboard pattern (left) juxtaposed with the NanEye camera image of the checkerboard pattern (right) to illustrate the severity of spherical aberration. **(b)** The pair of images depict the target of concentric circles (left) with a processed image captured by the NanEye camera (right) during data collection.

2.4 Animal Studies

All animal work was performed under an IACUC approved protocol. We used the total of 5 New Zealand White Rabbits. Anesthesia was induced using ketamine/xylazine followed with isoflurane. The rabbits were kept in their natural prone position. In each test, the sensor was placed on the eye of the anesthetized rabbit. A real-time image viewer installed on a PC was used to position the sensor so that the pupil was centered. Following this initial adjustment, the sensor remained in position for the duration of data collection. The image processing program was initiated, and to demonstrate acquisition of pupillary reflexes, we applied a sequence of stimulating white light pulses. In a typical experiment, white light was on for 10 seconds, and then subsequently off for 10 seconds. NIR light (non-stimulating) was on the entire time to provide illumination for image acquisition. Following data collection, the rabbits were returned to their cages.

Figure 3. Anesthetized New Zealand white rabbit outfitted with the functioning and illuminated pupillometer during a test trial.

3. DATA & RESULTS

3.1 Spherical Aberration

Imaging evaluations with checkerboard patterns demonstrated that significant spherical aberration existed as a result of the NanEye camera lens. The extent of the spherical aberration differed between set-up configurations. For (A), the sensor placed directly on a paper target, the aberration was most pronounced. The trend was roughly linear up to a physical radius of approximately 2.5 mm. The field of view was greater with this model, yielding a viewing distance of approximately 7.5 mm outward from the center point. When the plano-convex lens representative of the human eye was added between the target and the sensor (B), the severity of spherical aberration appeared to decrease. However, the field of view also decreased, with maximal FOV radius as 5.5 mm. For the configuration involving PVA applied between the sensor and lens (C), the correlation between physical radius and imaged radius is approximately linear. The field of view is further diminished, with the maximum measurable radius as 4.5 mm from the center of the image. For the configuration with the camera mounted through the corneal shield and placed directly against the representative lens and immersed in PVA (D), the correlation is linear. The maximum field of view is the lowest of the configurations, with 3mm as the maximal radius from the center of the image.

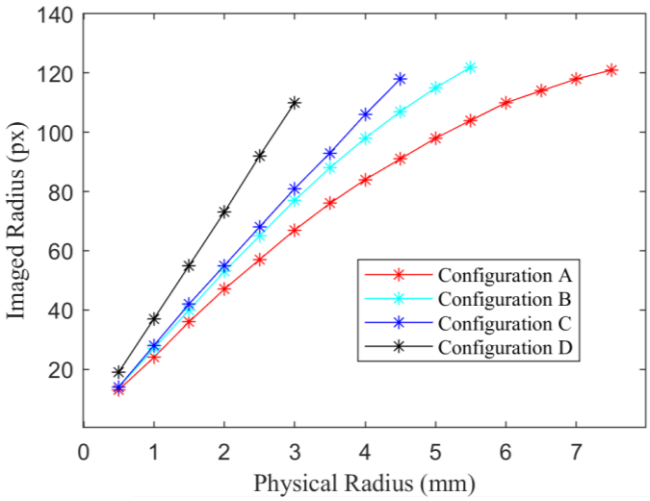

Figure 4. Analysis of spherical aberration for pupillometer test configurations with (A) the sensor centered on a printed target with air space as the interface, (B) the senor placed atop a plano-convex lens of 25 mm focal length on a target with an air interface, (C) the sensor atop the lens on the target with the interface between the lens and sensor occupied by PVA, and (D) the camera placed through the corneal shield via a small hole such that the camera rested on the plano-convex lens, immersed in PVA, which was placed upon a target.

3.2 Animal Studies

The images were processed as acquired to yield the pupil diameter, resulting in a near real-time display of the pupil diameter vs. time. From this information, the velocity at which the pupil constricts can also be extracted. The function yielded by the spherical aberration model (C) was then applied to the pixel diameters of the pupil. Figure 5 denotes the changes in pupil diameter over consecutive ten-second intervals of white light stimulation followed by ambient light.

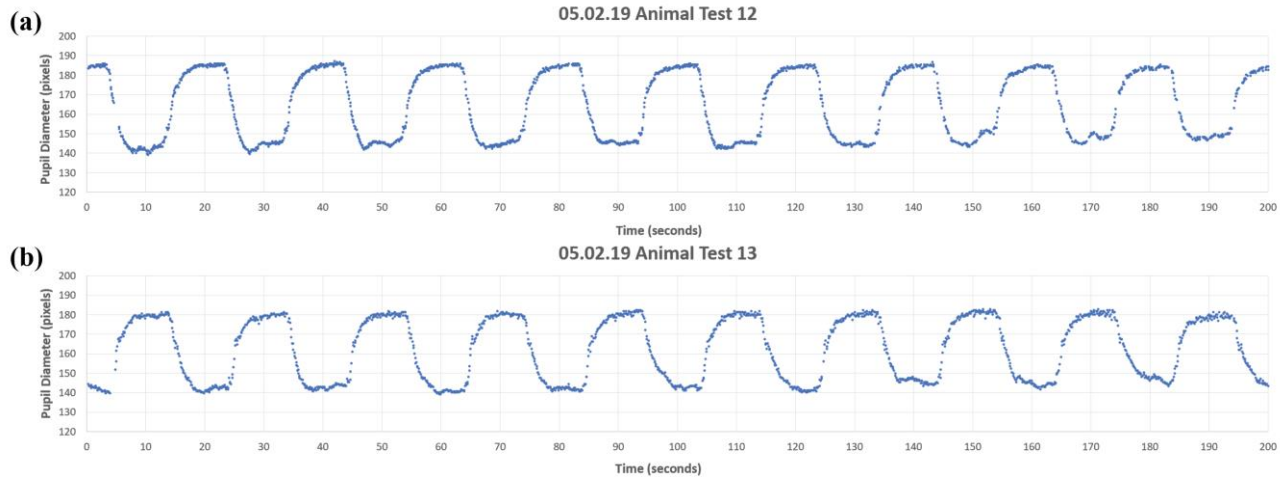

Figure 5. **(a) & (b)** Data reflecting real-time capture of pupil diameter in New Zealand white rabbits with regular intervals of 10-seconds-on, 10-seconds-off light stimulus captured by pupillometer.

We observed a reproducible pattern of constrictions and dilation, and recorded data for rate of constriction. From configuration (C), representative values for pupil diameter can be determined. For a fully constricted pupil experiencing white light stimulation with a measured diameter of 140 pixels, the physical diameter is approximately 5 mm. Conversely, a pupil exposed to solely ambient room lighting rests at 185 pixels in diameter, which can be translated to 7 mm. These measurements fall between the pupil range for a New Zealand white rabbit, 5-11 mm, noting that tests were conducted in a room with ambient light.[7]

4. CONCLUSION & DISCUSSION

The novel pupillometer presented here will enable investigation of cranial nerve injury and intracranial pressure elevation. These applications represent currently unmet medical needs in quantitative and minimally invasive methods of physiological monitoring of neurological conditions associated with brain injuries or neurosurgical procedures. Following animal tests, it is worth noting that the standard for measuring pupillary response generally involves shorter pulses of stimulation than were utilized for this study. The result is a lack of diameter saturation in standard models and therefore a slightly different waveform. In contrast, the 10-second on, 10-second off procedure allowed for the test pupil to reach diameter saturation every cycle. Working toward future IRB approval and first-in-human demonstration, the device will be tested in preclinical models. Based on our experience and available data, we expect that the pupillometer will assist in monitoring damage to cranial nerve II and III during anterior skull base procedures. Similarly, we expect to establish quantitative correlations between PLR and ICP in animal model. We have successfully demonstrated a pupillometer capable of continuous monitoring of PLR, with real-time extraction of quantitative data, and have explored the affects of varying interfaces on data collection.

ACKNOWLEDGMENTS

This work was supported by the Asset Development Award UA15-141 from Tech Launch Arizona to MR and ML. Technology described here has been disclosed in U.S. Patent Application No. 62/286,052, filed January 22, 2016. BS acknowledges a SPIE student travel award to present this work at Photonics West 2020.

REFERENCES

[1] Centers for Disease Control and Prevention, “TBI: Get the Facts | Concussion | Traumatic Brain Injury | CDC Injury Center,” U.S. Dep. Heal. Hum. Serv., 2019, <https://www-cdc-gov.ezproxy4.library.arizona.edu/traumaticbraininjury/get_the_facts.html> (8 January 2020).

[2] McGillicuddy, J.E., “Cerebral protection: Pathophysiology and treatment of increased intracranial pressure,” Chest 87(1), 85–93 (1985).

[3] Bhardwaj, A., Ellegala, D.B., and Kirsch, J.R., Eds., [Acute Brain and Spinal Cord Injury : Evolving Paradigms and Management] , CRC Press, Boca Raton (2008).

[4] Smith, M.M., Citerio, G.G., and Kofke, W.A.I., Eds., [Oxford Textbook of Neurocritical Care] , First, Oxford University Press USA - OSO, Great Britain (2016).

[5] Alexandridis, E., [The Pupil] , Springer-Verlag, New York (1985).

[6] St. Joseph Health, “Clinical Guidelines: Pupillometer in Critical Neuro Patients, Use of II. GENERAL INFORMATION OF DOCUMENT” (2015).

[7] Tsonis, P.A., [Animal Models in Eye Research] , in Anim. Model. Eye Res. (2008).